Electronic Supplementary Information

From ultrafast events to equilibrium - uncovering the unusual dynamics of ESIPT reaction. The case of dually fluorescent diethyl-2,5-(dibenzoxazolyl)-hydroquinone.

Paweł Wnuk,[a,]*Gotard Burdziński,[b] Michel Sliwa,[c] Michał Kijak,[a] Anna Grabowska,[a] Jerzy Sepioł,[a] Jacek Kubicki,[b,*]

[a] Institute of Physical Chemistry, Polish Academy of Sciences, Kasprzaka 44/52, Pl-01-224 Warsaw, Poland

[b] Faculty of Physics, Adam Mickiewicz University in Poznań, Umultowska 85, 61-614 Poznań, Poland

[c] Laboratory of Infrared and Raman Spectroscopy (LASIR) UMR 8516/CNRS Lille University 1, Lille, France

Corresponding author:
jacek.kubicki@amu.edu.pl; pwnuk@ichf.edu.pl

Figures and Tables captions

1. Experimental techniques

1a. Stationary spectra

Stationary absorption spectra were measured on JASCO-V550 spectrophotometer. Fluorescence spectra were recorded with the TCSPC system which can also work as a typical spectrofluorometer. In such configuration, instead of the time between excitation and the emission of first photon (TCSPC technique) the total numbers of photons per second vs. wavelength were measured. In this case the signal from the photomultiplier was sent directly to the photon counter. Additionally, the picosecond laser was used as a quasi-stationary source of the excitation light (4 MHz repetition rate).

1b. Chemicals

The diethyl-2,5(dibenzoxazolyl)-hydroquinone (DE-BBHQ)[1] was kindly given to us by professor J. M. Kaufmann from Philadelphia College of Pharmacy, USA. The sample was purified by chromatography and checked with NMR and UV spectra. The molar extinction coefficients determined at $S_0 \rightarrow S_1$ absorption maximum in CCl_4 and C_2Cl_4 are equal: 2.24×10^4 $M^{-1}cm^{-1}$ at 416 nm and 2.12×10^4 $M^{-1}cm^{-1}$ at 418 nm, respectively. Quantum yield (η_f) of the total fluorescence of DE-BBHQ was also measured using BBHQ in 3-MP as reference.[2] The η_f =0.021 and 0.024 in CCl_4 and C_2Cl_4, respectively (λ_{ex} =400 nm).

Solvents: dichloromethane (DCM), Merck, HPLC grade; tetrachloromethane (CCl_4), Merck, for spectroscopy; 1,2-dichloroethane (DCE), Aldrich, HPLC grade; tetrachlorethylene: (C_2Cl_4) (UV/IR) grade, Roth and Sigma-Aldrich, anhydrous 99%; tetrahydrofuran (THF), Sigma-Aldrich, anhydrous 99.9%; heptane (HEP), Sigma-Aldrich, anhydrous 99%; acetonitrile (ACN), Sigma-Aldrich, HPLC grade.

1c. Femtosecond UV/VIS and IR spectrometers

The ultrafast infrared laser system consists of a short-pulse titanium-sapphire oscillator (Coherent, Vitesse, 50 fs) followed by a high-energy titanium-sapphire regenerative amplifier (Coherent, Positive Light, Legend HE USP).[3] The 800 nm beam is split into two beams to generate second harmonic in BBO crystal (400 nm generation) and to pump OPA (Optical Parametric Amplifier, OPerA Coherent). The OPA with a DFG (Difference Frequency Generation) module generates IR pulses (tunable from 2 to 10 μm, 5 μJ at 4 μm). A Ge

beamsplitter splits the IR beam into reference and probe beams and both are focused into a 1 mm path length sample cell (Harrick Scientific), but only the probe beam overlaps with the pump beam in the sample. After passing through the sample the probe and reference beams were spectrally dispersed in a grating spectrometer (Horiba, iHR 320) and independently imaged on a liquid nitrogen cooled HgCdTe detector (2 × 32 elements) with 17 nm resolution. To avoid any interferences with residual absorption of water vapors, IR beams are permanently purged with dry air. Every other UV pump pulse is blocked by a synchronized chopper to eliminate long-term drift effects. The pump pulse energy was about 2 μJ at the sample position.

The broadband UV/VIS femtosecond transient absorption system has been described elsewhere.[4,5] The sample concentration was adjusted for an optical density of 1 at the excitation wavelength with a 1 mm path length. A sample volume of 50 mL was continuously flowed through the sample cell to ensure that fresh sample was photoexcited. The entire set of pump-probe kinetics is recorded at least three times, to ensure data reproducibility. To avoid rotational diffusion effects, the angle between polarizations of the pump beam and the probe beam was set to the magic angle (54.7°). Kinetic traces are analyzed by fitting to a sum of exponential terms. Convolution with a Gaussian response function is included in the global fitting procedure. The instruments response was approximately 300 fs Full Width at Half Maximum (FWHM). All experiments were performed at room temperature.

1d. Time Correlated Single Photon Counting (TCSPC) spectrometer

The time correlated single photon counting (TCSPC) system has been described elsewhere.[6] Briefly, spectrometer consists of the picosecond titanium–sapphire laser oscillator (Tsunami, Spectra Physics), pumped by Millennia Prime. Repetition rate of the picosecond oscillator (1.5 ps pulse duration) was reduced to 4 MHz using a electrooptical pulse picker. The second harmonic (400 nm) was generated by focusing fundamental beam onto surface of a BBO nonlinear crystal. The excitation beam was then focused in the sample by a quartz lens. The excitation beam intensity was adjusted by a rotating neutral filter to eliminate the photon pile-up effect. The emission polarizer was set at the magic angle in respect to vertical polarization of the excitation beam. The monochromator of the focal length 300 mm and aperture f/4.2 was equipped with a diffraction grating of 1800 grooves/mm. Optical signal was registered with proximity type 6 μm microchannel plate MCP-PMT R3809U-05 (Hamamatsu,

thermoelectrically cooled to −20°C), equipped with a high speed preamplifier C5594 (Hamamatsu). Electronic signal pathway was composed of an upgraded constant fraction discriminator CFD TC 454 (Tennelec), time to amplitude converter TAC-TC 864 (Tennelec), and a multichannel analyzer Norland 5000 MCA. The time per channel determined by the optical method was 0.61±0.01 ps. The full width at half maximum of IRF was about 30 ps. All experiments were performed at room temperature in non degassed solutions.

1e. Femtosecond up-conversion spectrometer

For fluorescence measurements with femtosecond time resolution we used up-conversion spectrometer, similar to one described in Ref. 7. It consists of femtosecond Ti:Sapphire oscillator (Coherent Mira, 110 fs, 80 MHz), followed by home build regenerative amplifier (5 kHz repetition rate, 1 mJ). Amplified pulses were split into two parts by a beam splitter, one part was used to generate second harmonic beam at 400 nm (utilizing BBO nonlinear crystal), while the rest of the pulse was send to Noncollinear Optical Parametric Amplifier (NOPA). Central wavelength of the pulses generated by NOPA was set at 1020 nm with compressed pulse energy of 10 μJ. Excitation beam at 400 nm was focused with a quartz lens on cuvette with 200 μm sample thickness. Fluorescence induced by excitation pulse was collected with all reflective Schwarzschild objective and imaged onto surface of BBO nonlinear crystal. Infrared pulses from NOPA which served as a ultrafast gate, were send through a delay stage and were mixed with fluorescence signal inside nonlinear BBO crystal. Up-converted signal was then routed to a imaging spectrometer (Andor, SR-303i), equipped with EM-CCD camera (Hamamatsu C9100-13). Spectrum for each delay between pulses was recorded many times to increase signal to noise ratio. Scattered excitation beam, which would saturate camera, was blocked by a color filter before an up-conversion process. A number of dispersive elements (such as: color filter, cuvette cover glass, solvent and BBO gating nonlinear crystal) in a fluorescence beam path results in a wavelength dependent group delay. A precise value of dispersion introduced by mentioned elements was determined independently with a white light interferometric spectrometer. Measured fluorescence evolution map was then corrected for measured group delay, with achieved temporal correction accuracy better than 5 fs in range of 400-700 nm. Setup was used with two different up-converting BBO crystals i.e. 0.2 mm – for high temporal resolution measurements (IRF=160 fs FWHM) and 2 mm thick crystal – for detection of weak signal with

reduced temporal resolution (IRF=450 fs FWHM). In the first case, temporal resolution was limited by excitation pulse duration, while in the second case it was determined by group velocity mismatch in a thick up-converting crystal. Accuracy of retrieved decay time constants in our case, are limited by a noise of recorded data, in practice accuracy was not worse than ±10%. For all experiments, polarization between excitation and gate beam was set at a magic angle configuration – to avoid rotational and diffusional effects of molecular motions.

2. Computational methods

All computations were done within the Gaussian 09 suite of programs.[8] The geometry optimizations for the ground (S_0) and the first electronically excited singlet state (S_1) were performed using the Density Functional Theory (DFT) and its time dependent (TD-DFT) formalism, respectively. The B3LYP hybrid functional and the 6-31+G(d,p) basis set were applied.

The potential energy profiles for the proton transfer reactions were obtained as a potential energy scan (PES) along the so-called coordinate-driven reaction path (CDRP, all coordinates are optimized except one, appropriately chosen, which is fixed and varied systematically). The fixed coordinate was the longer of the O-H and N-H distances in a hydrogen bond with a translocating proton. For the double proton transfer C2h symmetry of the system was preserved along the path (concerted symmetric reaction). The real transition states were also localized, with the use of the TS Gaussian 09 option. Vibrational frequency analysis performed for all of the localized stationary points, confirmed their minimum/saddle point nature.

The calculations, which included the presence of a solvent, used a Polarizable Continuum Model (PCM) in its state-specific implementation. Full geometry optimization in solution was performed for the ground state, whereas for the excited S_1 state vacuum geometry was used. Non-equilibrium solvation energies of the vertically excited states have been calculated to obtain vertical excitation energies in solution.

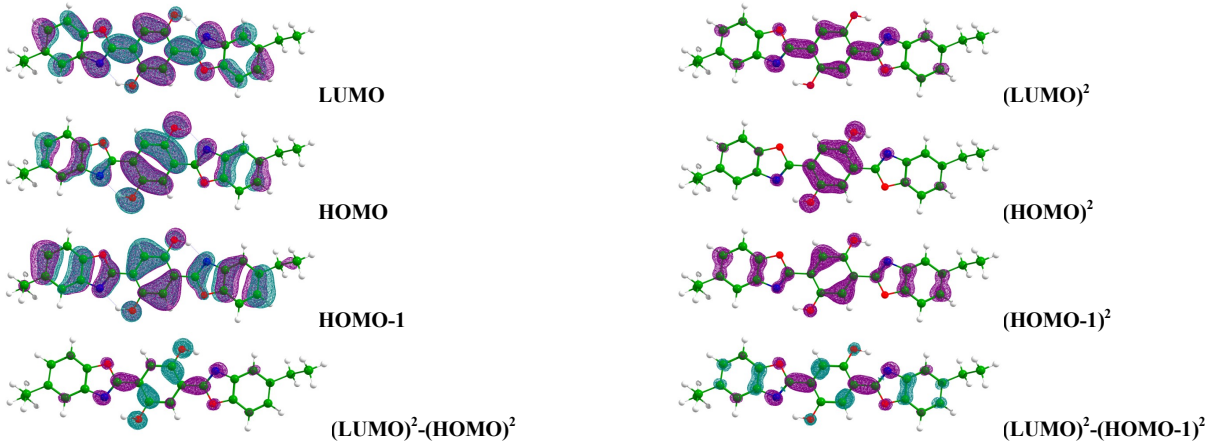

Figure S1. Isosurfaces of electron density (left part) or its square (right part) of the lowest unoccupied orbital (first row) and two highest occupied ones (second and third row) calculated at the DFT level. At the bottom, respective differences, illustrating density changes accompanying the two lowest electronic transitions in DE-BBHQ are presented.

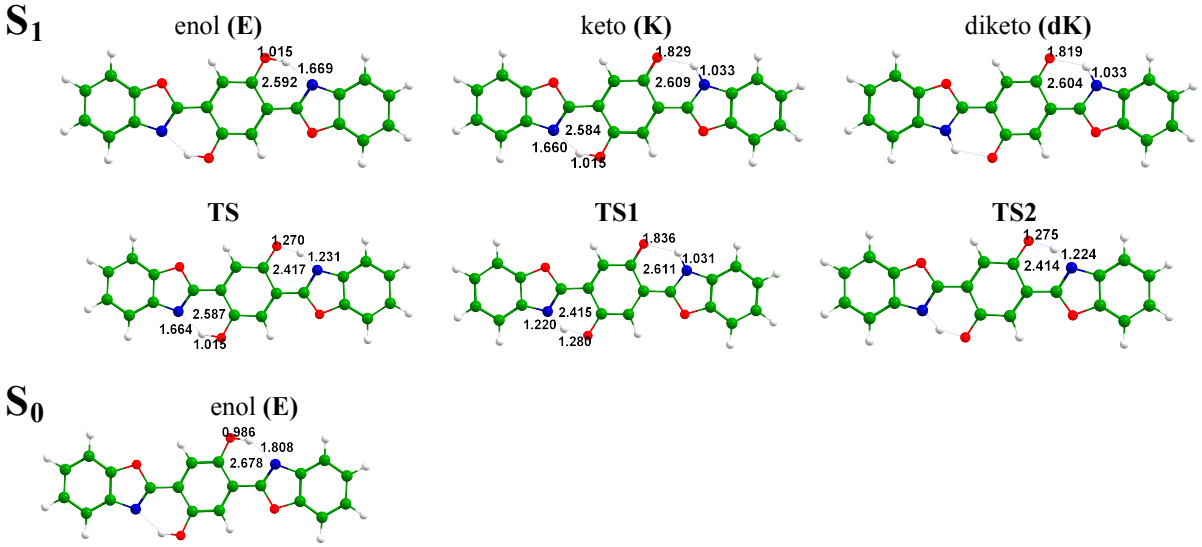

Figure S2. Optimized geometries of different possible tautomers of BBHQ and transition states (see Figure S3) between them in the ground (S_0) and the first excited state (S_1) calculated at the DFT level. Relevant hydrogen bond distances (in Å) are given by numbers (r_{OH}, r_{NH}). The distance between ON (r_{ON}) is also given (the higher value).

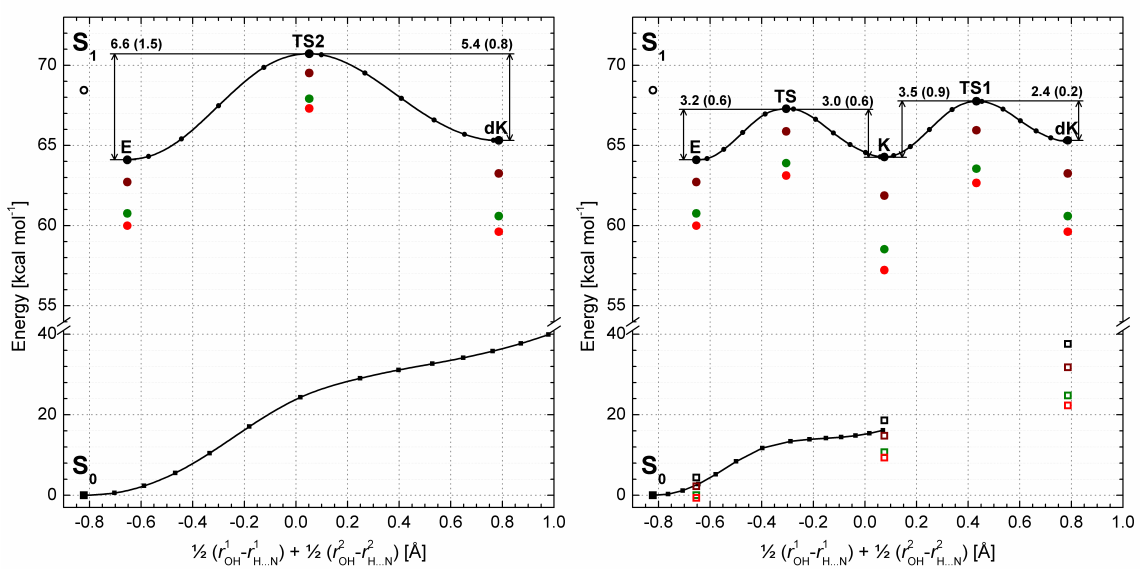

Figure S3. The S_0 (full squares) and the S_1 (full circles) potential energy profiles along the synchronous concerted (left) or the stepwise (right) double proton transfer reaction paths in BBHQ calculated at the DFT level (r^1 and r^2 refers to the first and second proton coordinates for double proton transfer reaction). Energies of the S_1 stationary points recalculated in solutions (hexane/THF/acetonitrile brown/green/red symbols, respectively) for the S_1 (solvent in equilibrium) and vertical the S_0 states (non-equilibrium solvation condition) are also presented (full circles and open squares, respectively). Barrier heights (in kcal/mol) are given by numbers (in brackets, after ZPE correction). For the second step of the stepwise reaction the potential energy profile for the ground state was not calculated since there is no stable keto structure in S_0.

Table S1. Relative energies of different tautomeric forms and transition states between them in the S_1 optimized state ($E_{S1}/\Delta E_{S1}/\Delta E_{S1\ ZPE}$) and vertically excited the S_0 state (E_{S0}), solvation energies (E_{solv}), dipole moments (μ), vertical excitation energies (Ex), oscillator strengths (f) and relative fluorescence intensities under equilibrium conditions ($I_i \backslash I_{total}$) of BBHQ/DE-BBHQ in vacuum and in solutions calculated at the DFT level.

			E_{S1} [kcal/mol]	$E_{solv\ S1}$ [kcal/mol]	ΔE_{S1} [a] [kcal/mol]	$\Delta E_{S1\ ZPE}$ [a, b] [kcal/mol]	μ_{S1} [D]	E_{S0} [kcal/mol]	$E_{solv\ S0}$ [kcal/mol]	μ_{S0} [D]	$Ex_{S1\rightarrow S0}$ [cm^{-1}]	$f_{S1\rightarrow S0}$	I_i/I_{total} [c]
BBHQ	vacuum	**E**	**64.10**		**0.00**	**0.00**	**0.00**	**4.43**		**0.00**	**20870**	**0.431**	**0.619**
		TS	**67.29**		**3.18**	**0.64**	**2.24**	**14.95**		**1.48**			
		K	**64.28**		**0.18**	**0.05**	**5.24**	**18.60**		**2.51**	**15980**	**0.238**	**0.369**
		TS1	**67.76**		**3.66**	**0.98**	**2.74**	**31.38**		**0.68**			
		dK	**65.32**		**1.21**	**0.78**	**0.00**	**37.61**		**0.00**	**9690**	**0.145**	**0.012**
		TS2	**70.72**		**6.62**	**1.53**	**0.00**	**26.62**		**0.00**			
	hexane	**E**	**62.72**	**-1.38**	**0.00**	**0.00**	**0.00**	**2.25**	**-2.19**	**0.00**	**21150**	**0.432**	**0.218**
		TS	**65.88**	**-1.41**	**3.16**	**0.61**	**2.74**	**12.07**	**-2.88**	**1.74**			
		K	**61.87**	**-2.41**	**-0.85**	**-0.97**	**6.38**	**14.81**	**-3.79**	**3.02**	**16460**	**0.242**	**0.764**
		TS1	**65.95**	**-1.81**	**3.23**	**0.55**	**3.33**	**26.71**	**-4.67**	**0.91**			
		dK	**63.25**	**-2.07**	**0.53**	**0.09**	**0.00**	**31.78**	**-5.83**	**0.00**	**11010**	**0.156**	**0.018**
		TS2	**69.52**	**-1.21**	**6.80**	**1.71**	**0.00**	**22.94**	**-3.67**	**0.00**			
	THF	**E**	**60.76**	**-3.34**	**0.00**	**0.00**	**0.00**	**0.05**	**-4.38**	**0.00**	**21230**	**0.429**	**0.025**
		TS	**63.90**	**-3.39**	**3.14**	**0.59**	**3.50**	**9.07**	**-5.88**	**2.22**			
		K	**58.53**	**-5.75**	**-2.24**	**-2.36**	**8.00**	**10.70**	**-7.90**	**4.17**	**16730**	**0.247**	**0.965**
		TS1	**63.55**	**-4.21**	**2.79**	**0.11**	**4.12**	**21.41**	**-9.97**	**1.57**			
		dK	**60.59**	**-4.73**	**-0.17**	**-0.61**	**0.00**	**24.79**	**-12.82**	**0.00**	**12520**	**0.170**	**0.010**
		TS2	**67.91**	**-2.81**	**7.15**	**2.06**	**0.00**	**18.93**	**-7.68**	**0.00**			
	acetonitrile	**E**	**59.99**	**-4.11**	**0.00**	**0.00**	**0.00**	**-0.65**	**-5.08**	**0.00**	**21210**	**0.426**	**0.010**
		TS	**63.12**	**-4.17**	**3.13**	**0.58**	**3.82**	**8.09**	**-6.85**	**2.44**			
		K	**57.22**	**-7.06**	**-2.78**	**-2.90**	**8.64**	**9.35**	**-9.25**	**4.67**	**16740**	**0.248**	**0.984**
		TS1	**62.66**	**-5.10**	**2.67**	**-0.01**	**4.42**	**19.60**	**-11.78**	**1.86**			
		dK	**59.62**	**-5.70**	**-0.38**	**-0.81**	**0.00**	**22.32**	**-15.29**	**0.00**	**13050**	**0.176**	**0.006**
		TS2	**67.31**	**-3.41**	**7.32**	**2.22**	**0.00**	**17.59**	**-9.03**	**0.00**			
DE-BBHQ	vacuum	**E**	**64.08**		**0.00**	**0.00**	**0.00**	**4.41**		**0.00**	**20870**	**0.501**	**0.589**
		K	**64.18**		**0.10**	**-0.04**	**5.49**	**18.44**		**2.66**	**16000**	**0.264**	**0.392**
		dK	**64.99**		**0.90**	**0.47**	**0.00**	**37.08**		**0.00**	**9760**	**0.160**	**0.019**
	hexane	**E**	**62.79**	**-1.29**	**0.00**	**0.00**	**0.00**	**2.20**	**-2.21**	**0.00**	**21190**	**0.506**	**0.198**
		K	**61.87**	**-2.31**	**-0.92**	**-1.06**	**6.57**	**14.62**	**-3.81**	**3.15**	**16520**	**0.270**	**0.774**
		dK	**62.98**	**-2.01**	**0.18**	**-0.26**	**0.00**	**31.24**	**-5.84**	**0.00**	**11100**	**0.172**	**0.028**
	acetonitrile	**E**	**60.23**	**-3.85**	**0.00**	**0.00**	**0.00**	**-0.84**	**-5.25**	**0.00**	**21360**	**0.509**	**0.009**
		K	**57.39**	**-6.80**	**-2.85**	**-2.99**	**8.66**	**9.04**	**-9.40**	**4.69**	**16910**	**0.280**	**0.979**
		dK	**59.36**	**-5.63**	**-0.87**	**-1.31**	**0.00**	**21.70**	**-15.38**	**0.00**	**13170**	**0.195**	**0.012**

[a] relative to the enol form in a given environment

[b] zero point vibrational energy corrected values (vibrational energy scaled by 0.964)

[c] calculated according to $I_i/I_{total} = g_i \times \exp(-E_i/(k \times T)) \times Ex_i^2 \times f_i / \Sigma_i (g_i \times \exp(-E_i/(k \times T)) \times Ex_i^2 \times f_i)$, where: g – degeneracy (equal 1 for **E** and **dK** and 2 for **K**), k –Boltzmann constant, T – temperature (298 K), $E = \Delta E_{S1\ ZPE}$ and summation covers **E**, **K** and **dK** forms

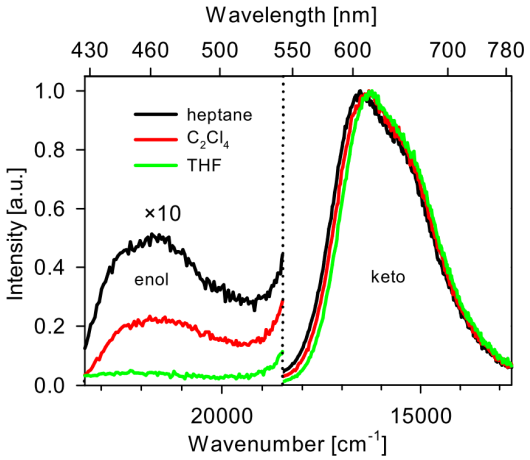

Figure S4. Steady state fluorescence spectra of DE-BBHQ (λ_{exc}=400 nm). Relative intensity of the excited enol tautomer in various solvents. The emission bands of keto tautomer were normalized to the same amplitude.

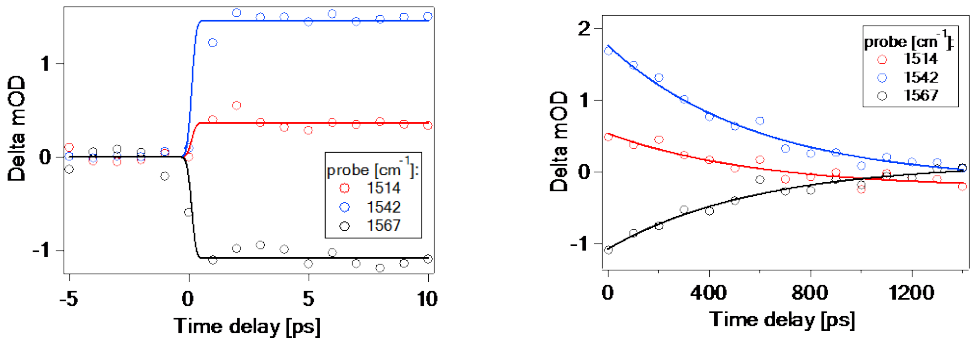

Figure S5. Femtosecond measurements in the IR range: selected kinetics of DE-BBHQ in C_2Cl_4 at 1514, 1542 and 1567 cm^{-1} at short (a) and at long time scale (b).

Table S2. Kinetic parameters obtained with UV/VIS transient absorption technique.

Wavelength [nm]	A_1	τ_1	A_2	τ_2 [ps]	A_3	τ_3 [ps]	offset
430	-0.048	0.25	—	—	-0.033	271	-0.003
490	-0.049	0.18	—	—	0.031	383	0.002
650	0.041	0.33	0.003	7.7	-0.018	365	0.000

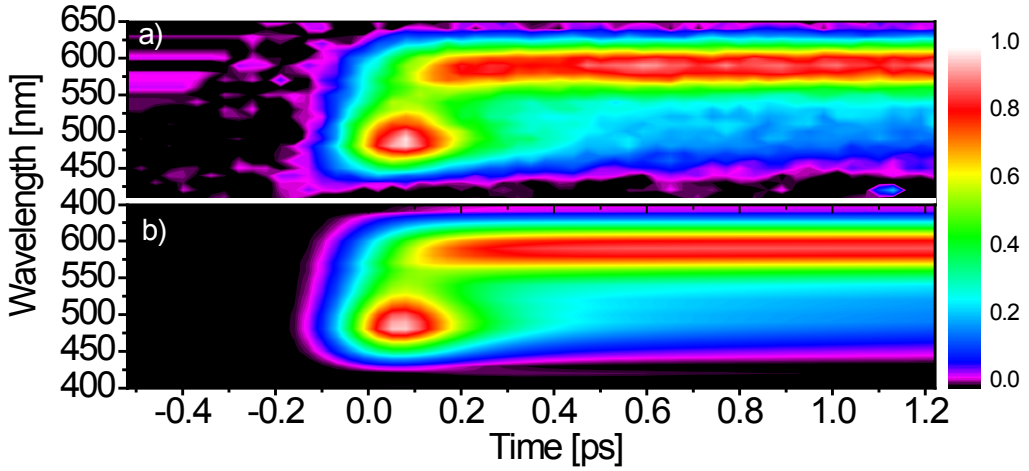

Figure S6. Registered time resolved fluorescence spectra of DE-BBHQ in C_2Cl_4 using up-conversion setup - a), compared with reconstructed map - b), using parameters of the fit obtained with global analysis.

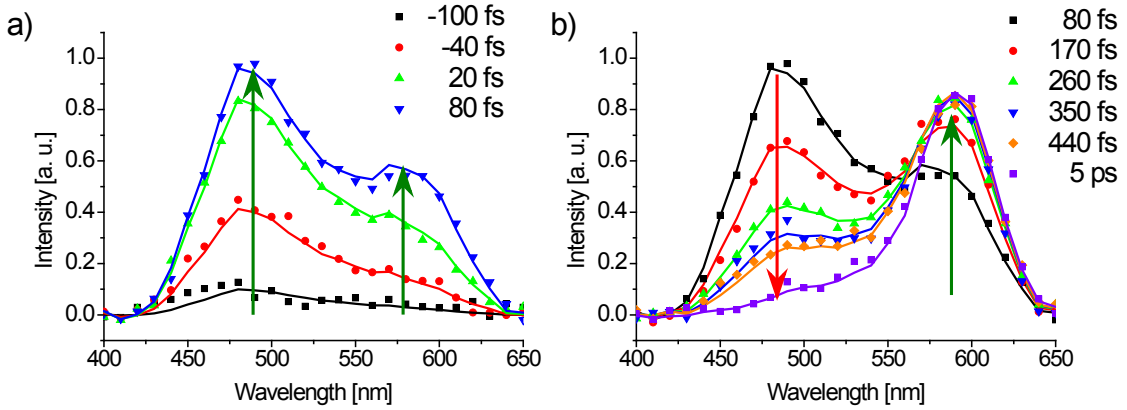

Figure S7. Fluorescence of DE-BBHQ in C_2Cl_4 at different time delays after excitation pulse, (a) the rise of both forms, (b) the decay of enol with simultaneous rise of keto form.

References

1. J. M. Kauffman, G. S. Bajwa, *J. Heterocyclic Chem.* 1993, **30**, 1613.
2. A. Mordziński, A. Grabowska, W. Kuehnle, A. Krówczynski, A. *Chemical Physics Letters* 1983, **101**, 291.
3. G. Burdzinski, M. Sliwa, Y. Zhang, S. Delbaere, *The Journal of Physical Chemistry A* 2011, **115**, 14300.
4. G. Buntinx, R. Naskrecki, O. Poizat, *The Journal of Physical Chemistry* 1996, **100**, 19380.
5. M. Sliwa, N. Mouton, C. Ruckebusch, L. Poisson, A. Idrissi, S. Aloise, L. Potier, J. Dubois, O. Poizat, G. Buntinx, *Photochemical & Photobiological Sciences* 2010, **9**, 661.
6. T. Wróżowa, B. Ciesielska, D. Komar, J. Karolczak, A. Maciejewski, J. Kubicki, *Review of Scientific Instruments* 2004, **75**, 3107.
7. B. Białkowski, Y. Stepanenko, M. Nejbauer, C. Radzewicz, J. Waluk, *Journal of Photochemistry and Photobiology A: Chemistry* 2012, **234**, 100.
8. M. J. Frisch, G. W. Trucs, H. B. Schegel, Wellingford CT: **2009**.